Application of GWFAP to real micro-terrain wind fields in Fujian Province

Hongjie Zhang [1, a], Fengli Yang [1, b], Ziqiang Tang [2, c], Huixue Dang [3, d], Yitong Cheng [4, e]

[1]China Electric Power Research Institute, Beijing, 100055, China
[2] Fujian Electric Power Economic Research Institute, Fuzhou, Fujian, China
[3] School of Civil Engineering, Chang'an University, Xi'an, Shaan'xi, China
[4] North China Electric Power University, 102206, Beijing, China

[a] 75790868@qq.com, [b] 23995064@qq.com, [c] 398715837@qq.com
[d] huixuedang@aliyun.com, [e] 417701029296@163.com

Abstract. The wind fields around micro-terrain in ultra-high voltage transmission line is analysed by using GWFAP (general wind flow analysis platform). The micro-terrain zone is extracted and selected from ASTER GDEM V2 database, and mixed prism-tetrahedron meshes is generated for the inner zone. Then structured grid sharing the same node height at two zone interfaces is constructed and then converted to unstructured mesh. The B type wind profile with 13m/s different reference wind speed at 10m height is applied to inlet boundary and the wind profile at tower location is obtained. This whole process is automatically carried out and great effort is saved comparing to manual operations.

Key words: Transmission lines; real micro-terrain; wind field; GWFAP.

1. Introduction

The natural source in western region of China is usually converted to electric power and then transmitted by transmission line to east China. Thus, transmission line is constructed, and it usually pass through wide mountain regions with complex topography. In mountainous regions, the atmospheric wind flow is greatly altered from standard wind profiles due to heat transfer as well as topography variation when it passes upon undulating hills and hilly areas [1]. Thus, local flow characteristics will be evidently different from the result captured by meteorological station, and the buildings and constructions designed based on the standards and codes of plat ground may be destructed due to local strong winds [2]. However, the commonly used standards and codes rarely describe the local flow induced by mountain regions due to its locality characteristics, including sharp change of elevation, temperature, and deep-cutting gorge.

Accounting for the above problem, local wind field analysis should be carried out. In the published literatures, Daniel S. Abdi [3] et al. pointed out that, real topography contains irregular three-dimensional topographic features which are surrounded by other topographic features, thus this difference often leads to overly conservative design of structures constructed on complex terrain. This problem is more pronounced for long span structures such as transmission line towers that cross the crest of hills and escarpments, where the fractional speed up ratio can be highly enough to cause major structural failures. For this problem, many national standards and codes, such as NBCC, ASCE-7, AS/NZS 1170.2, EUROCODE 1, etc., provide genal guidelines for estimating topographical multiplication factors of wind speed-up over hill crests and escarpments. However, the guidelines presented in the above codes are tested and proposed for simple hilly geometries. While for complex mountain zones, all these codes suggested wind tunnel tests and CFD simulations for wind load validations.

Due to the massiveness as well as complexity of terrain topology in the wide geophysical range that transmission line across, it is very expensive to test many micro-terrain wind fields by using wind tunnel tests. Thus, CFD simulation can be of nice choice. However, for huge number of micro-terrains, it is time-consuming and dull to manually generate mesh, setting boundary conditions, submitting cases, post-processing results [4]. Thus, automatic integrated platform for wind flow analysis is very favorable and several researchers have attributed their work.

Automatic generation of mesh over complex geometries is the most difficult problem. In present study, mixed unstructured tetrahedron and prism meshes are adopted to discretize computational zones. This is due to that, automatic mesh generation by using these elements are not fully resolved caused by the defect of topology division of quadrilaterals and hexagons. But unstructured tetrahedron mesh generation is well developed and it is widely employed in industrial analysis. E.g. Muller [5] et al. combined advancing front method and Delaunay method together for unstructured surface mesh generation. Frey [6] developed it to be three dimensional and it was found to be with both the high-quality characteristic of advancing front method and the high efficiency and convergence characteristics of Delaunay method. In the most recent years, WU Huo-zhen[7] and Jonathan Richard Shewchuk[8] investigated 3D constrained Delaunay triangulation algorithm based on the classical 3D Delaunay tetrahedral mesh generation method, and they found that constrained Delaunay tetrahedralizations maintain most of the favorable properties of ordinary Delaunay tetrahedralizations, but some sets of constraining segments and facets simply do not have constrained Delaunay tetrahedralizations. This problem is fixed by and boundary conformity can always be enforced by judicious insertion of additional vertices, combined with constrained Delaunay tetrahedralizations. Daming Feng [9] et al. presented a scalable three-dimensional hybrid parallel Delaunay image-to-mesh conversion algorithm (PDR.PODM) for distributed shared memory architectures, which could highly improve the efficiency of unstructured mesh geneartion. David Eller [10] combines the Delaunay-based tetrahedral mesh generator TETGEN and a novel technique for creation of a prismatic layer together, thus an open source implementation of an efficient mesh generation procedure for hybrid prismatic-tetrahedral meshes intended for use in Reynolds-averaged Navier-Stokes solutions is developed.

These published literatures in unstructured mesh generation can be nice reference in automatic grid generation, however, for transmission lines cross different mountainous zones, the geometry model is difficult to be built manually. Thus, the GDEM data from ASTER GDEM V2 is employed in the construction of geometry model, and then mixed tetrahedron/prism meshes are generated. Then the boundary conditions are applied by using scripts. Finally, data extraction will also be carried out by using scripts.

During bridge construction and wind energy development [14], a large number of CFD simulation studies have been carried out for the mountainous microtopographic wind field, which provides a feasible way to obtain the characteristics of mountainous wind field and design parameters of transmission lines. Based on the above research results, this paper carries out the simulation analysis of complex microtopographic flow field, and obtains the corresponding relation between wind direction and acceleration ratio of wind speed; meanwhile combined with direction of transmission lines, it further analyzes the impact of complex topography on the wind load of transmission lines.

2. zone selection of micro-terrain

The research object of microtopography is the location of transmission lines in the first mountain range offshore Fujian coast. Use Google Earth to obtain elevation data of topography undersurface, take samples spaced by 30m and totally obtain 43,381 discrete elevation points, and import the discrete elevation points into the reverse engineering software Global mapper to fit the four-terraced terrain surface. The surface 3D modeling is shown in Figure 1. Spaced by 15°, select 24 angles of direction wind for CFD simulation analysis, and line trend is 48° north by east. Figure 2 shows the spatial position relation among tower position, line trend, and angle of direction wind.

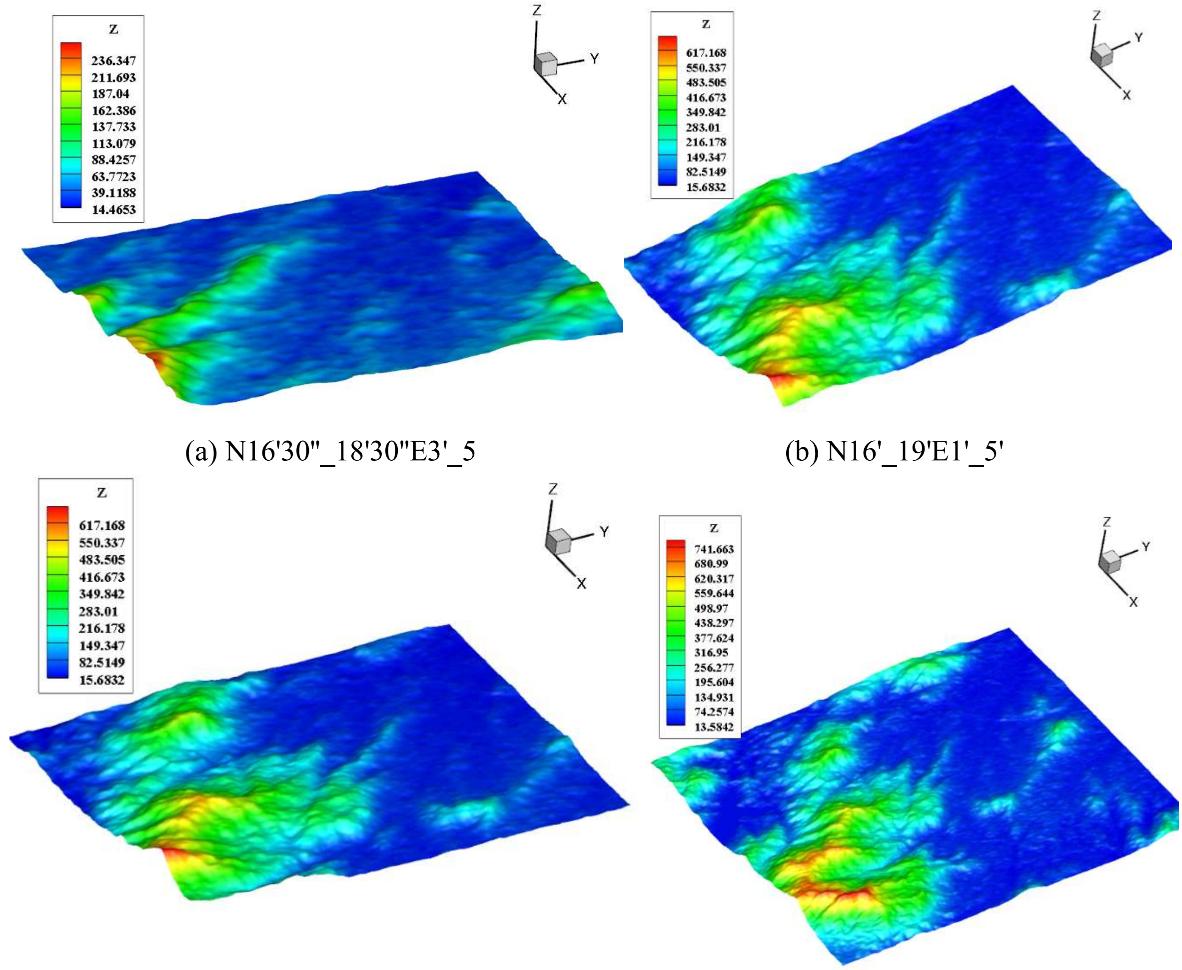

(a) N16'30"_18'30"E3'_5 (b) N16'_19'E1'_5'

(c) N15'40"_19'20"E1'_5' (d) N14'_20'E0'_6'

Figure 1. Height contour corresponding to different longitude and latitude ranges

3. Research of Regularity of Acceleration Ratio of Wind Speed in True Wind Field

Delaunay method is employed for both surface mesh and volume mesh generation. Prism layers are generated based on surface mesh on the terrain and ground surface meshes. In order to guide air flow smoothly from plat ground to miro-terrain, smooth blending technique is used. Then prism mesh is generated based on surface triangular mesh. To avoid self-interaction of prism mesh elements, the technique proposed by David Eller[10] is employed. Tetrahedral mesh is then generated by using Delaunay method based on the upper most triangular surface mesh of prism layers. The surface mesh on interface cylinder is triangular mesh for tetrahedron elements, while for prism layers, its surface mesh on interface cylinder is quadrilateral. The surface mesh of inner rotational domain is shown in Figure 2.

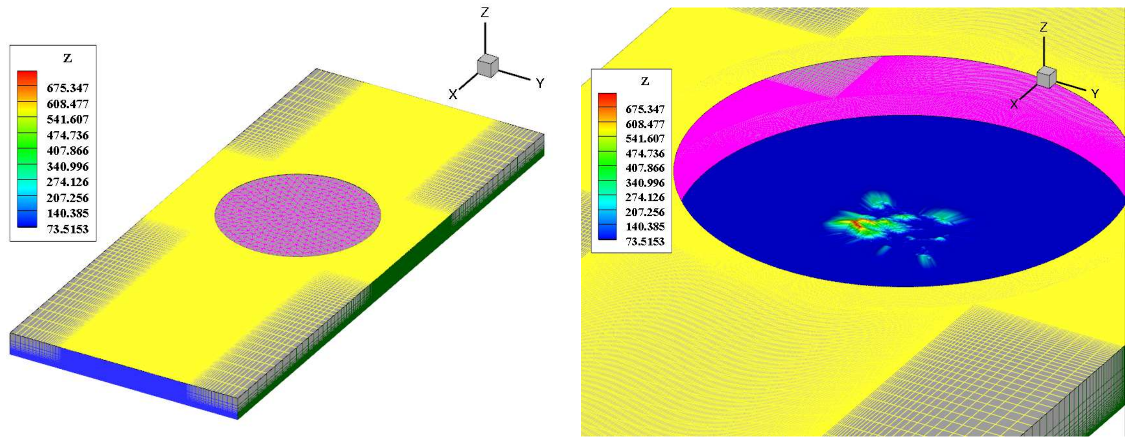

(a) surface mesh (b) height contour of micro-terrain

Figure 2. Surface mesh of inner rotational region

Accounting for wind angle variation, the computational domain is divided into two parts: a) inner rotational domain and b) outer zone, as shown in Figure 3, by referring to the rotational gauge in test section of wind tunnel.

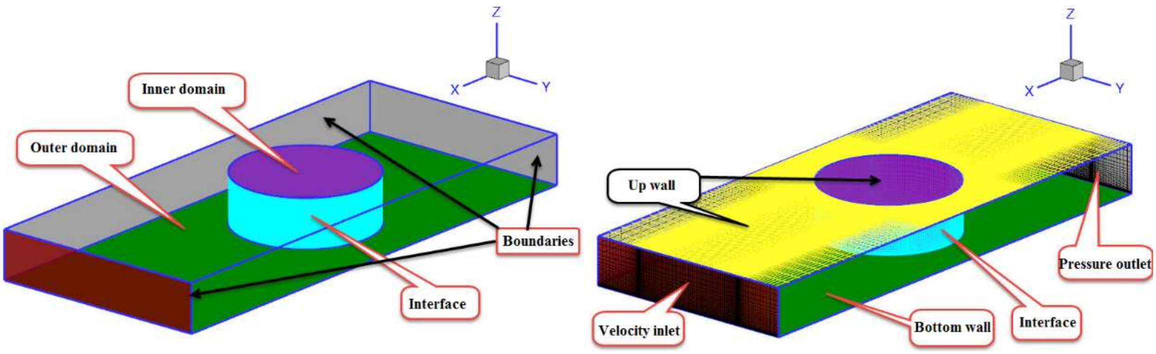

(a) Domains and boundaries (b) Boundary conditions

Figure 3. computational domains and boundary conditions

4. Research Wind profile and wind incidence

Wind profile at inlet boundary is selected to be one of the A, B, C, D type. It is expressed as:

$$V_z = V_{10}\left(\frac{z}{10}\right)^{\alpha} \tag{1}$$

where α is to be 0.12, 0.15, 0.22, and 0.30, respectively.

The turbulence intensity profile is expressed as follows:

$$\bar{I}(z) = \left(\frac{z}{z_s}\right)^{-\alpha} \tag{2}$$

The turbulence kinetic energy profile is written as:

IOP Conf. Series: Materials Science and Engineering **452** (2018) 032040 doi:10.1088/1757-899X/452/3/032040

$$k(z)=\frac{\sigma_u^2(z)+\sigma_v^2(z)+\sigma_w^2(z)}{2}\cong\sigma_w^2(z)=\left(I(z)U(z)\right)^2 \tag{3}$$

The turbulence dissipation rate is written as:

$$\varepsilon\cong P_k(z)\cong-\overline{u'w'}\frac{dU(z)}{dz}\cong C_\mu^{1/2}k(z)\frac{dU(z)}{dz} \tag{4}$$

The dominant wind incidence angle is determined by that of wind rose map shown in Figure 4, e.g., the wind incidence step can be determined to be 5 degree in the wind angle range of 30 degree to 75 degree.

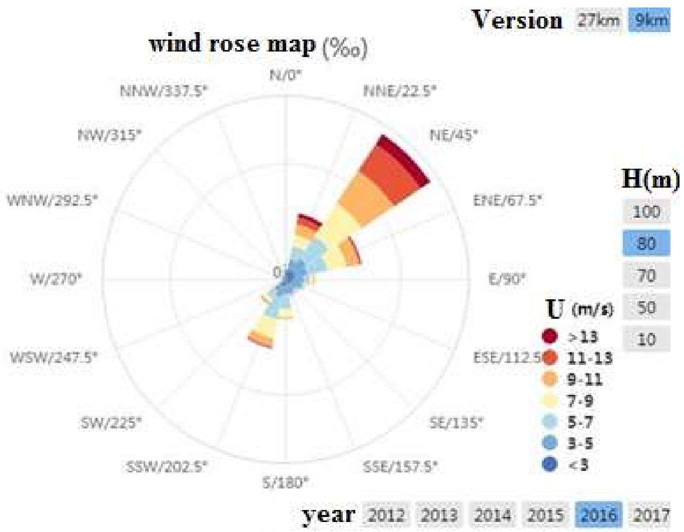

Figure 4. wind rose map of local terrain

5. Some Numerical Results

Numerical simulations are conducted at different wind angle, and wind profiles at different locations are extracted. The unstructured mesh of micro-terrain is shown in Figure 5, with local refinement carried out to capture local geometry variance.

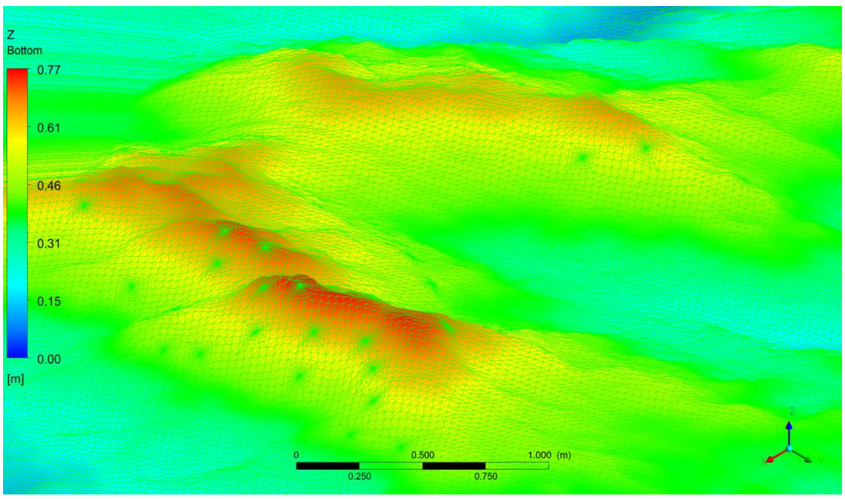

Figure 5. Surface Mesh of Micro-Terrain with Local Refinement

doi:10.1088/1757-899X/452/3/032040

The wind pressure contour at different wind angle are shown in Figure 6.

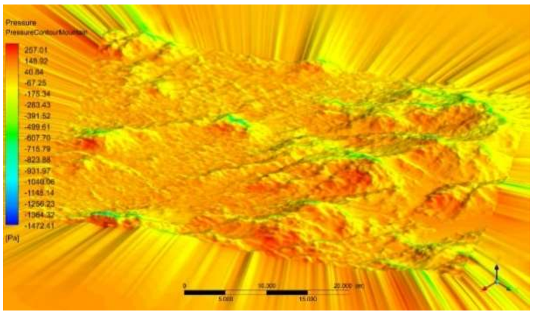
(a) 30° wind angle

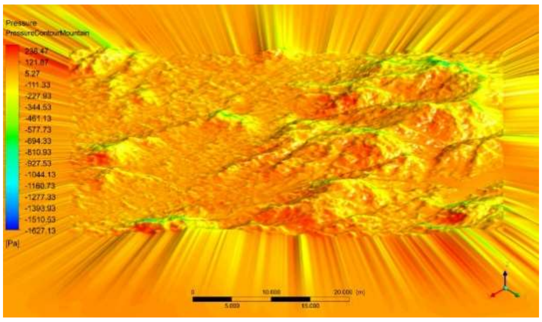
(b) 45° wind angle

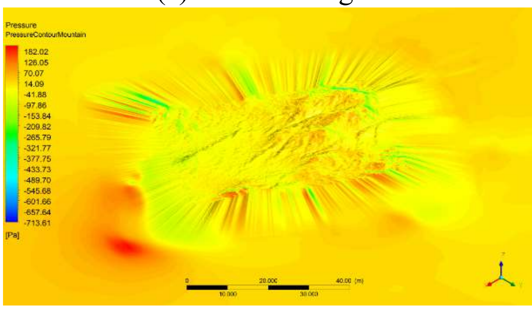
(c) 60° wind angle

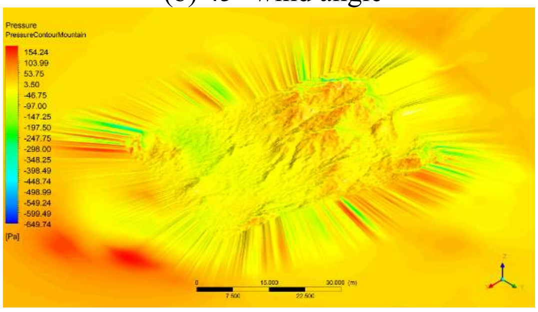
(d) 75° wind angle

Figure 6. Surface Pressure Contours of Micro-Terrain at Different Wind Angles

Some extracted wind profiles at (E118.0595, N24.2881) are plotted as shown in Figure 7. Its height and wind speed are normalized by using reference height 10m and reference wind speed at 10m, respectively.

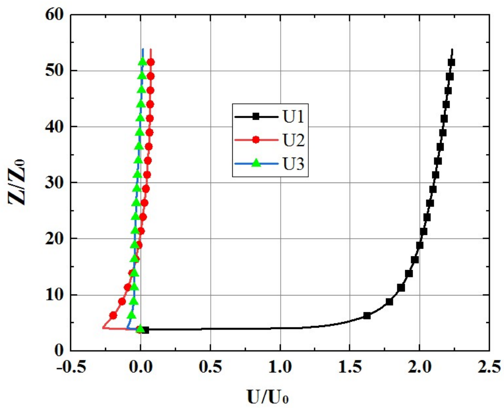

(a) 30° wind angle

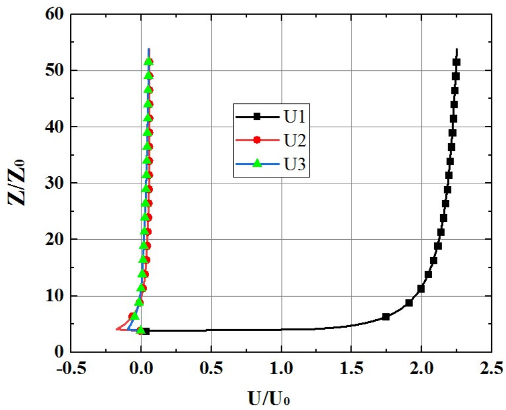

(b) 45° wind angle

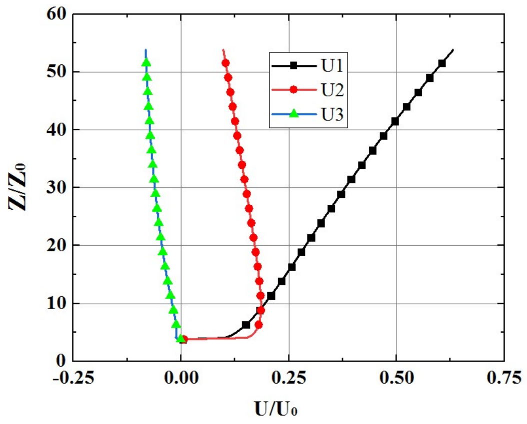

(c) 60 wind angle

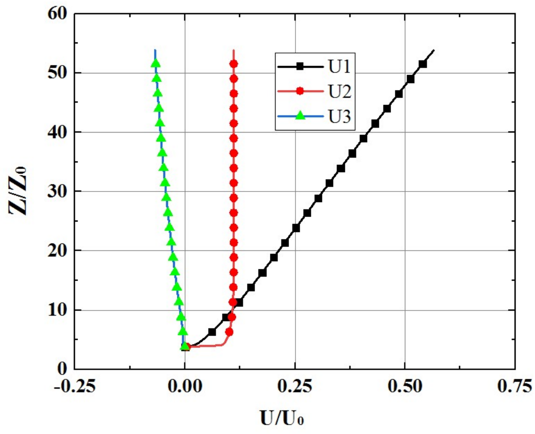

(d) 75° wind angle

Figure 7. Wind Profiles of Micro-Terrain at Different Wind Angles

6. Conclusion

By using the GWFAP, the wind field of micro-terrain in Fujian province is simulated. The wind angles are selected to be the dominated wind angle. Surface pressure contours are plotted and wind profiles normalized by using reference height(10m) and reference wind speed (U at 10m height) is plotted. The results indicate that, wind profile of micro-terrain is strongly dependent on wind angle. For this micro-terrain, the wind speed is strongly much larger at 30°, 45°, than those at 60°, 75°. The wind speed acceleration ratio is greater than 2.0 for the cases of 30°, 45° wind angles. Attention should be paid for these wind angles for wind resist analysis of transmission towers in the zone of local micro-terrain.

Acknowledgments

This work has been funded by the State Grid Corporation of China (Project name: High Resolution Wind Field Characteristics Study on Mountainous Terrain by Adaptive Simulation Technology), and the financial aid number is GCB17201600017. The authors would like to thank the sponsor of State Grid Corporation of China.

References

[1] LU Qian. *Study on Wind Turbine Distribution in Complex Geology*. [J] *Shanghai Power*. 2008,(06):513-515.

[2] ZHOU Zhi-yong, XIAO Lian, DING Quan-sun, et al. *Numerical Simulation Study of Wind Environment for the Flow around Large Region with Complex Terrain.* [J] *Chinese Quarterly of Mechanics*, 2010,31(1):101-107.

[3] Daniel S. Abdi, Girma T. Bitsuamlak. *Wind flow simulations on idealized and real complex terrain using various turbulence models.* [J] *Advances in Engineering Software*, 75 (2014): 30–41.

[4] Qiang Du, DeshengWang. *Recent progress in robust and quality Delaunay mesh generation.* [J] *Journal of Computational and Applied Mathematics,* 195 (2006):8-23.

[5] J.D.Muller, P.L.Roe, H. Deconinck. *A Frontal Approach for Node Generation in Delaunay Triangulations.* [J] *International Journal for numerical Methods in Engineering,* 1993,17(3):241-255.

[6] P.J.Frey, Houman Borouchaki, Paul-Louis George. *3D Delaunay Mesh Generation Coupled with an Advancing Front Approach.* [J] *Computer Methods in Applied Mechanics & Engineering*, 1998, 157:115-131.

[7] WU Huo-zhen, JIAO Yu-yong, LI Hai-bo, et al. *Study of 3D finite element tetrahedral mesh automatic generation for complex regions.* [J] *Rock and Soil Mechanics*, 2011,32(11):3479-

3486.

[8] Jonathan Richard Shewchuk. *Constrained Delaunay Tetrahedralizations and Provably Good Boundary Recovery.* [J] *Eleventh International Meshing Roundtable*, 2002:193-204.

[9] Daming Feng, Christos Tsolakis, Andrey N. Chernikov. *Scalable 3D Hybrid Parallel Delaunay Image-to-Mesh Conversion Algorithm for Distributed Shared Memory Architectures.* [J] *Procedia Engineering*, 124 (2015):18-30.

[10] David Eller, Maximilian Tomac. *Implementation and evaluation of automated tetrahedral-prismatic mesh generation software[J]. Computer-Aided Design,* http://dx.doi.org/10.1016;j.cad.2015.06.010.